Nanomanufacturing and Metrology (2020) 3:228–235
https://doi.org/10.1007/s41871-020-00069-0

ORIGINAL ARTICLE

Remote Absolute Roll-Angle Measurement in Range of 180° Based on Polarization Modulation

Xiuguo Chen[1] · Jinbao Liao[1] · Honggang Gu[1] · Chuanwei Zhang[1] · Hao Jiang[1] · Shiyuan Liu[1]

Received: 13 April 2020 / Revised: 27 June 2020 / Accepted: 29 June 2020 / Published online: 30 July 2020

Abstract

Remote measurement of object orientation is often required in many applications. Out of the six degrees of freedom (DoF) that determine object orientation in space, the roll angle is the most difficult to measure using optical methods. In this letter, we propose a remote Stokes roll-angle sensor that measures roll angles from the detected Stokes vectors of modulated polarized light retroreflected from a sensing unit comprised simply of a retarder and a planar reflection mirror. Experimental results have shown that the proposed sensor can realize absolute roll angle measurement in an unprecedented range of 180° with a maximum absolute error of less than 0.25° and a measurement resolution of better than 0.01°. The proposed sensor adopts a coaxial design and takes the advantages of compactness, simplicity and low cost, and moreover, can be further expanded to a three-DoF angle sensor due to the sensitivity of the sensing unit to other two kinds of angles (pitch and yaw).

Keywords Roll angle · Angle sensor · Polarization modulation · Stokes polarimeter

1 Introduction

Knowledge of orientation of a remote object plays a crucial role in many applications ranging from space missions, scientific research to industrial applications, such as autonomous docking of two spacecrafts [1], torsion balance for laser interferometer gravitation-wave observatory [2], and navigation of robots [3]. Six DoF (three positions and three angles) are required to completely determine the orientation of an object in space. Position and angle measurements can be carried out in an incremental manner or in an absolute manner. Compared with the incremental approach, absolute measurement in a large range is important to improve the efficiency and robustness of precision positioning systems, since it does not require initialization to obtain the absolute orientation at startup and is immune to emergency events causing inaccurate accumulation such as unexpected interrupt [4].

Out of the six DoF, the roll angle that describes a rotation around the longitudinal axis has long been deemed to be the most difficult to measure. Several techniques have been developed for measuring roll angle [5]. Among these techniques, a common method to realize remote roll angle measurement is to use a retroreflector and analyze phase difference [6, 7] or displacement difference [8] between the reference and retroreflection beams or intensity ratio between *p*- and *s*-polarizations of the retroreflection beam [9]. Nevertheless, it should be noted that this method is primarily suitable for incremental measurement within a small range. In comparison, the polarization-based measurement can provide a high sensitivity in a relatively large measuring range. Li et al. presented a compact roll-angle sensor working in range of 30° with 0.01° resolution by using a Faraday rotator to modulate polarization direction of the probe light [10]. Gillmer et al. further improved the roll-angle sensor in [10] to a 43° working range with

✉ Xiuguo Chen
xiuguochen@hust.edu.cn

Jinbao Liao
jinbaoliao@hust.edu.cn

Honggang Gu
hongganggu@hust.edu.cn

Chuanwei Zhang
chuanweizhang@hust.edu.cn

Hao Jiang
hjiang@hust.edu.cn

Shiyuan Liu
shyliu@hust.edu.cn

[1] State Key Lab of Digital Manufacturing Equipment and Technology, Huazhong University of Science and Technology, Wuhan, China

0.002° resolution by replacing the Faraday rotator therein with an acousto-optic modulator [11]. We recently presented a roll-angle sensor that could realize absolute angle measurement in range of 180° from the detected Stokes vector of the modulated polarized light transmitted through a quarter-wave plate acting as the sensing unit [12]. However, it is noted that the above polarization-based roll-angle sensors [10–12] are not well suited for remote measurement, since the light emitting and receiving (detecting) units must be arranged on two sides of the sensing unit.

In this paper, we propose a remote Stokes roll-angle sensor that can realize absolute angle measurement in a range of 180°. Compared with our previous work [12], two major contributions have been made in this work. First, the system layout of the Stokes roll-angle sensor is improved to make it more suitable for remote measurement. In the proposed roll-angle sensor, a retarder and a planar reflection mirror compose the sensing unit, where the retarder modulates the roll angular displacement into the change of state of polarization (SoP) of the probe polarized light and the reflection mirror acts as the retroreflector so that the light emitting and receiving units can be arranged on the same side. A Stokes polarimeter is employed to detect the Stokes vector of the SoP of the modulated polarized light retroreflected from the sensing unit. We propose a self-calibration method to calibrate system parameters of the sensor by fitting measured Stokes elements to the theoretically calculated data according to an established model of the sensor system based on Stokes–Mueller formalism. Second, a least squares regression (LSR) method is proposed to estimate roll angles from the detected Stokes vectors, which is shown to achieve a higher accuracy than the calculation method using only one of the Stokes elements in [12].

2 Measurement Principle

Figure 1 presents the schematic of the remote Stokes roll-angle sensor, which consists of two units, namely the emitting/receiving unit and the sensing unit. The emitting/receiving unit is composed of a polarized light source, a non-polarizing beamsplitter (NPBS), and a Stokes polarimeter. The sensing unit, which is composed of a sensing retarder (SR) and a planar reflection mirror (RM), is fixed with a rotating component under test and is used to modulate the SoP of light beam from the incoming linear polarization to the outcoming elliptical polarization. The outcoming elliptically polarized light finally enters into a Stokes polarimeter, which is used to collect the Stokes vector of the polarized light. The Stokes vector consists of four elements

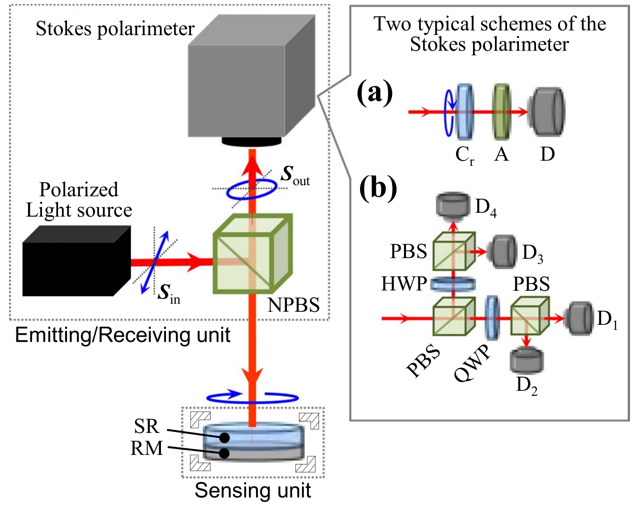

Fig. 1 (Color online) (*Left*) Schematic of the remote Stokes roll-angle sensor, where NPBS, non-polarizing beamsplitter; *SR* sensing retarder; *RM* reflection mirror. (*Right*) Two schemes of the Stokes polarimeter. **a** Rotating-retarder polarimeter, where Cr, rotating retarder; *A*, analyzer; *D*, detector; **b** four-channel polarimeter, where *PBS*, polarizing beamsplitter; *HWP*, half-wave plate; *QWP*, quarter-wave plate; D_1–D_4, detectors 1–4

$$\boldsymbol{S} = \begin{bmatrix} S_0 \\ S_1 \\ S_2 \\ S_3 \end{bmatrix} = \begin{bmatrix} I_p + I_s \\ I_p - I_s \\ I_{+45^\circ} - I_{-45^\circ} \\ I_{\mathrm{R}} - I_{\mathrm{L}} \end{bmatrix}, \tag{1}$$

which can describe the SoP of any polarized light. Here, I_p and I_s are light intensities of *p*- and *s*-polarizations, respectively (the *p*–*s* axes as well as the wave vector constitute a right-handed orthogonal coordinate that is conventionally used to describe light polarizations); I_{+45° and I_{-45° are light intensities of $+45°$ and $-45°$ linear polarizations, respectively (with respect to *p*–*s* axes); I_{R} and I_{L} are light intensities of right- and left-circular polarizations, respectively. The measuring roll angle can be finally obtained from the measured Stokes elements.

According to the Stokes–Mueller formalism, the Stokes vector $\boldsymbol{S}_{\mathrm{out}}$ of the elliptically polarized light entering into the Stokes polarimeter can be represented by

$$\boldsymbol{S}_{\mathrm{out}} = \mathbf{M}^{\mathrm{t}}_{\mathrm{BS}}\mathbf{M}_{\mathrm{SR}}(\delta, -\beta)\mathbf{M}_{\mathrm{RM}}\mathbf{M}_{\mathrm{SR}}(\delta, \beta)\mathbf{M}^{\mathrm{r}}_{\mathrm{BS}}\boldsymbol{S}_{\mathrm{in}}, \tag{2a}$$

where $\boldsymbol{S}_{\mathrm{in}} = [1, \cos(2\alpha_0), \sin(2\alpha_0), 0]^{\mathrm{T}}$ denotes the Stokes vector of the emitting light from the polarized light source with α_0 being the polarization direction angle; $\boldsymbol{S}_{\mathrm{out}} = S_0[1, s_1, s_2, s_3]^{\mathrm{T}}$ denotes the Stokes vector of the polarized light entering into the Stokes polarimeter and s_1, s_2 and s_3 are the normalized Stokes elements to the first element S_0; $\mathbf{M}_{\mathrm{SR}}(\delta, \beta) = \mathbf{R}(-\beta)\mathbf{M}_{\mathrm{SR}}(\delta)\mathbf{R}(\beta)$ with $\mathbf{M}_{\mathrm{SR}}(\delta)$ and $\mathbf{R}(\beta)$ being

$$\mathbf{M}_{SR}(\delta) = \begin{bmatrix} 1 & 0 & 0 & 0 \\ 0 & 1 & 0 & 0 \\ 0 & 0 & \cos\delta & \sin\delta \\ 0 & 0 & -\sin\delta & \cos\delta \end{bmatrix}, \tag{2b}$$

$$\mathbf{R}(\beta) = \begin{bmatrix} 1 & 0 & 0 & 0 \\ 0 & \cos(2\beta) & \sin(2\beta) & 0 \\ 0 & -\sin(2\beta) & \cos(2\beta) & 0 \\ 0 & 0 & 0 & 1 \end{bmatrix}, \tag{2c}$$

which represent the Mueller matrix of SR and the Mueller rotation transformation matrix, respectively. Here, δ and β are the retardance and fast-axis orientation angle of SR, respectively. Note that β can further be represented as $\beta = \beta_0 + \theta$, with β_0 and θ being the initial fast-axis orientation angle of SR and the measuring roll angle, respectively; $\mathbf{M}_{RM}$ is the Mueller matrix of RM, which is a diagonal matrix with diagonal elements being 1, 1, − 1, and − 1; $\mathbf{M}_{BS}^{r}$ and $\mathbf{M}_{BS}^{t}$ represent Mueller matrices of NPBS in the reflection and transmission modes, respectively. Although most commercial NPBSs declare to be non-polarizing, it has been found that the p- and s-polarizations after the NPBS still have a minor shift with each other in both reflection and transmission modes [13]. The residual polarization effect of NPBS should be taken into account for high-accuracy polarization measurement. Assume that the beamsplitter coating is only comprised of isotropic films, in the most general case, $\mathbf{M}_{BS}^{r/t}$ are given by

$$\mathbf{M}_{BS}^{r/t} = \begin{bmatrix} 1 & N_{r/t} & 0 & 0 \\ N_{r/t} & 1 & 0 & 0 \\ 0 & 0 & C_{r/t} & -S_{r/t} \\ 0 & 0 & S_{r/t} & C_{r/t} \end{bmatrix}, \tag{2d}$$

and $N_{r/t} = -\cos(2\Psi_{r/t})$, $C_{r/t} = \sin(2\Psi_{r/t})\cos(\Delta_{r/t})$, and $S_{r/t} = -\sin(2\Psi_{r/t})\sin(\Delta_{r/t})$, with $\Psi_{r/t}$ and $\Delta_{r/t}$ denoting the amplitude ratio and phase difference between p- and s-polarizations after polarized light reflected from or transmitted through the NPBS, respectively.

According to Eq. (2), the explicit expression of the normalized Stokes elements s_1, s_2 and s_3 with respect to the measuring roll angle θ can be obtained, which for brevity are simply expressed as

$$\left[s_1,\ s_2,\ s_3\right]^{T} = \boldsymbol{F}(\theta). \tag{3}$$

Assume that we have accurately known the system parameters α_0, β_0, δ as well as $\Psi_{r/t}$ and $\Delta_{r/t}$ (which need to be calibrated, as illustrated before), Eq. (3) only contains one unknown parameter, namely the measuring roll angle θ. In our previous work [12], θ was obtained from s_1 and meanwhile s_2 and s_3 were used to distinguish the interval of θ. In fact, θ can be obtained from any of the three expressions associated with s_1, s_2 and s_3, which indicates that Eq. (3) is an over-determined equation with three dependent variables and only one independent variable. Instead of acquiring θ from only one of the three normalized Stokes elements, we propose to obtain θ by solving an LSR problem such that

$$\hat{\theta} = \underset{\theta\in\Theta}{\arg\min} \left\| \left[s_1, s_2, s_3\right]_{\exp}^{T} - \boldsymbol{F}\left(\theta \middle| \alpha_0, \beta_0, \delta, \Psi_{r/t}, \Delta_{r/t}\right) \right\|, \tag{4}$$

where $\left[s_1,\ s_2,\ s_3\right]_{\exp}^{T}$ denotes the measured Stokes elements; $\boldsymbol{F}\left(\theta \middle| \alpha_0,\ \beta_0,\ \delta,\ \Psi_{r/t},\ \Delta_{r/t}\right)$ is the corresponding calculated Stokes elements with any roll angle θ and the known system parameters α_0, β_0, δ as well as $\Psi_{r/t}$ and $\Delta_{r/t}$; $\|\cdot\|$ denotes the vector norm; and Θ is the range of θ. Since the fast axis of SR after a 180° rotation coincides with that at its initial position, all Stokes elements have a period of 180°. Hence, the range of θ should be $\Theta \in [0°,\ 180°)$. Evidently, here the measurement of the roll angle is an absolute measurement since have known the initial fast-axis orientation angle β_0, of SR, which will keep constant after installation. For measuring s_1, s_2 and s_3, there are many types of available Stokes polarimeters [14]. The right side of Fig. 1 presents two commonly used schemes of the Stokes polarimeters, of which Fig. 1a, b correspond to the rotating-retarder polarimeter and the four-channel polarimeter, respectively. The rotating-retarder polarimeter has a simple layout and a compact size. In comparison, the Stokes roll-angle sensor based on a four-channel polarimeter is well suited for high-dynamic metrology, since the four Stokes elements are determined simultaneously in the four-channel configuration. In addition, attention should also be paid to the retardance δ of SR to obtain the roll angle. The SR cannot be a half-wave plate (i.e., $\delta = 180°$), since it can be demonstrated according to Eq. (2) that all Stokes elements will be constant with respect to θ when $\delta = 180°$.

3 Experiments

3.1 Experimental Setup

To demonstrate the performance of the proposed method in remote absolute roll-angle measurement, we have developed a prototype of the remote Stokes roll-angle sensor. As illustrated in Fig. 2, the polarized light source was comprised of a high-stability light source (EQ-99XFC, Energetiq Technology, Inc., USA) (not shown in the figure) and a linear polarizer (PGT5012, Union Optics, Inc., China). The light with a wavelength of 633 nm (other wavelength could also be chosen) was made to pass successively through the linear polarizer (P), the collimating lens (CL), the NPBS (UTB0020-4, Union Optics, Inc., China), the SR (a specially designed Quartz biplate with a retardance of ~ 138°), and was reflected by the RM (BB1-E02, Thorlabs, Inc., USA). The SR was

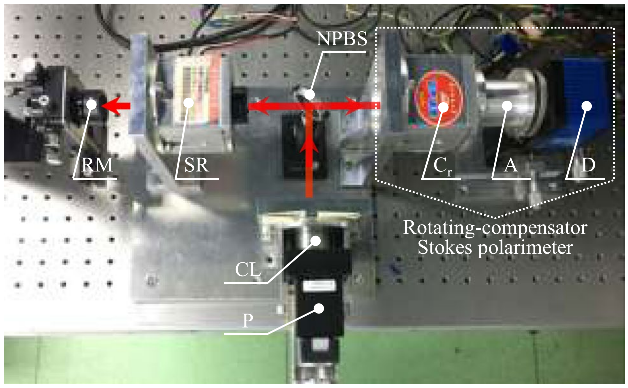

Fig. 2 (Color online) Prototype of the developed remote roll-angle sensor. *P*, linear polarizer; *CL*, collimating lens; *NPBS*, non-polarizing beamsplitter; *SR*, sensing retarder; *RM*, reflection mirror; *Cr*, rotating retarder; *A*, analyzer; *D*, detector

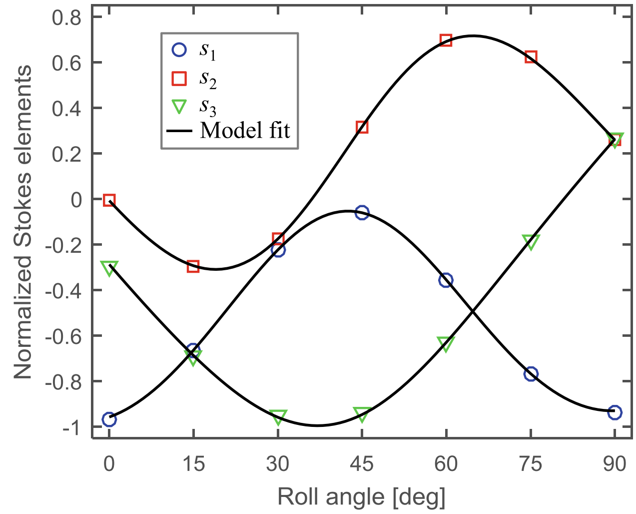

Fig. 3 (Color online) Fitting result between the measured and calculated best-fit normalized Stokes elements at different roll angles. The *discrete data points* correspond to the measured data, and the *solid line* corresponds to the calculated best-fit data

mounted in a hollow-shaft servo-motor (HO-63-A-44-A-E-000, Applimotion, Inc., USA) to simulate the rotation of the rotating component under test. The reflected light by the RM again pass through the SR, the NPBS, and finally entered into a home-made Stokes polarimeter developed based on a rotating-compensator configuration as shown in Fig. 1a (commercial Stokes polarimeters are also available).

It should be pointed out that the above components are identified just to specify the experimental setup adequately. Such identification is not intended to imply that these components are necessarily the best available for the purpose. Actually, the experimental setup shown in Fig. 2 was not specially designed but was revamped from a previous instrument in our lab [15], which thus makes the presented setup of the remote roll-angle sensor seem to be pretty large. By replacing current components, especially the employed servo-motors, with smaller ones, the size of the experimental setup can be further reduced. The measurement speed of the proposed remote roll-angle sensor depends on that of the employed Stokes polarimeter. The measurement time for the home-made rotating-compensator Stokes polarimeter is about 4 s. High-speed measurement can be achieved by using a multi-channel Stokes polarimeter [16], as illustrated in Fig. 1b. In addition, due to the limited space in our lab, we did not perform roll-angle measurement in remote distance. However, it can be noted from the measurement principle that the measurement distance is primarily limited by the beam divergence. Roll-angle measurement in very remote distance can be achieved with a highly collimated light beam.

3.2 Sensor Calibration

As described in Eq. (4), to acquire the measuring roll angle θ, it is prerequisite to calibrate the system parameters α_0, β_0, δ as well as $\Psi_{r/t}$ and $\Delta_{r/t}$. We adopted a self-calibration method by fitting the measured Stokes elements to the theoretically calculated data according to Eq. (2). To improve calibration accuracy, the sensing unit was rotated in a range from its initial orientation β_0 with a certain and precise increment in the calibration process. The measured Stokes elements associated with all the rotation orientations of the sensing unit as an ensemble were then fitted to the corresponding theoretically calculated Stokes elements. A mean-squared-error (MSE) function was adopted to estimate the fitting error between the measured and calculated Stokes elements in the fitting procedure, which is defined as

$$\mathrm{MSE}=\frac{1}{\sqrt{3M-K}}\left\{\sum_{j=1}^{M}\sum_{i=1}^{3}\left[\frac{s_{i,j}^{\mathrm{exp}}-s_{i,j}^{\mathrm{calc}}(\alpha_0,\beta_0,\delta,\Psi_{r/t},\Delta_{r/t})}{\sigma(s_{i,j})}\right]^2\right\}^{1/2}, \tag{5}$$

where M denotes the total number of rotated orientations of the sensing unit, K is the number of system parameters need to be calibrated (here $K=7$), $s_{i,j}^{\mathrm{exp}}$ and $s_{i,j}^{\mathrm{calc}}$ are the measured and calculated Stokes elements, respectively, and $\sigma(s_{i,j})$ are the standard deviations of the measured Stokes elements, which were estimated to be $\sigma(s_{i,j})=0.001$ for the developed Stokes polarimeter. The Levenberg–Marquardt algorithm [17] was adopted to solve the regression problem described above.

Figure 3 presents the fitting result between the measured and calculated best-fit Stokes elements at roll angles varied from 0° to 90° with an increment of 15°. Good agreement can be observed from Fig. 3, which yields an MSE of 6.61. The calibrated system parameters are $\alpha_0=48.63°$, $\beta_0=93.42°$, $\delta=138.00°$, $\Psi_r=-15.34°$, $\Delta_r=20.15°$, $\Psi_t=40.49°$, and $\Delta_t=-0.31°$, respectively. The retardance δ of SR as well as the amplitude ratios $\Psi_{r/t}$ and phase differences $\Delta_{r/t}$ of NPBS in reflection and transmission modes were also measured by a Mueller matrix ellipsometer (ME-L, Wuhan Eoptics Technology Co., China) and were found to be $\delta=137.91°$, $\Psi_r=38.05°$, $\Delta_r=17.6°$, $\Psi_t=39.9°$, and $\Delta_t=0.66°$, respectively, which agreed well with the above calibration values considering practical installation error.

4 Results and Discussion

Figure 4a presents the measured roll angles when the sensing unit rotates over 180° with an increment of 20° according to Eq. (4). The linear fitting yields a linear equation of $y=0.9997x+0.0500$ and a coefficient of determination of $R^2=1.0$, which indicate that the measured roll angles show a quite good linear relationship with respect to the input values. It thereby clearly demonstrates the capability of the proposed remote Stokes roll-angle sensor for absolute roll-angle

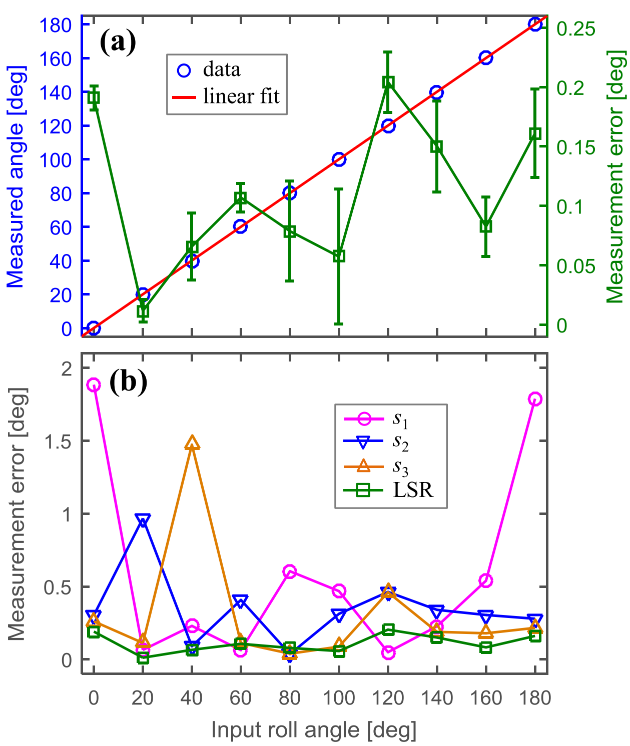

Fig. 4 (Color online) **a** Measured roll angles when the sensing unit rotates over 180° with an increment of 20° as well as absolute measurement errors between the input and measured roll angles. The associated error bars of the absolute measurement errors correspond to 30 repeated measurement uncertainties with a 95% confidence level; **b** Comparison of absolute measurement errors between the input and the measured roll angles from one of the three normalized Stokes elements (s_1, s_2, s_3) as well as by using the proposed LSR method

measurement in the range of [0°, 180°). The measurement errors between the input and measured roll angles are also presented in Fig. 4a, which are defined as the absolute differences between the input and measured roll angles. The associated error bars of the absolute measurement errors correspond to the repeated measurement uncertainties with a 95% confidence level. As can be observed, the measurement errors are less than 0.25° over the whole measuring range.

The measurement errors in the measured roll angles are primarily attributed to calibration errors of system parameters. As described above, the system parameters were calibrated by fitting the calculated Stokes elements to the measured data. Any errors in the measured Stokes elements will finally propagate to the calibrated parameters through the fitting procedure. The errors in the measured Fourier coefficients are mainly induced by random fluctuations in the detected light intensity and imperfect optical components (Note that Eqs. (2b) and (2d) just correspond to Mueller matrix models of perfect optical components). Further improvement of calibration accuracy is expected to lead to further decrease of measurement errors. Figure 4b also presents the comparison of absolute measurement errors between the input and measured roll angles from one of the three normalized Stokes elements as well as by using the LSR method as described in Eq. (3). Evidently, the LSR method exhibits a better performance than the approach by using only one of the three normalized Stokes elements.

The measurement resolution of the developed roll-angle sensor was tested by controlling the servo-motor rotated with different incremental steps. Considering that different input roll angles yield different measurement uncertainties, as revealed by Fig. 4a, we test the measurement resolution at different starting values. Figure 5a, b present the measured roll angles as a function of input roll angles with an increment of 0.02° starting from 0° and 100°, respectively. Figure 5c, d further present the testing results with an increment of 0.01° starting from 0° and 160°, respectively. The red dotted lines in Fig. 5 correspond to the means of 30 repeated measurement carried out for each increment of the input roll angles. As can be observed from Fig. 5, the difference between the means of adjacent incremental steps is different from the setting increment. This is primarily attributed to the fluctuation of the optical encoder of the employed servo-motor. The encoder resolution of the servo-motor is 288,000 counts/revolution. The actual fluctuation of the encoder is about ± 2 counts around the setting value, which corresponds to an uncertainty of the setting increment of about 0.0025°. Even so, as indicated by Fig. 5, the developed sensor can clearly distinguish input roll angles with a step of even less than 0.01°. It therefore suggests that the measurement resolution of the developed sensor should be better than 0.01°.

The measurement resolution of the developed sensor is mainly limited by the measurement precision of the Stokes

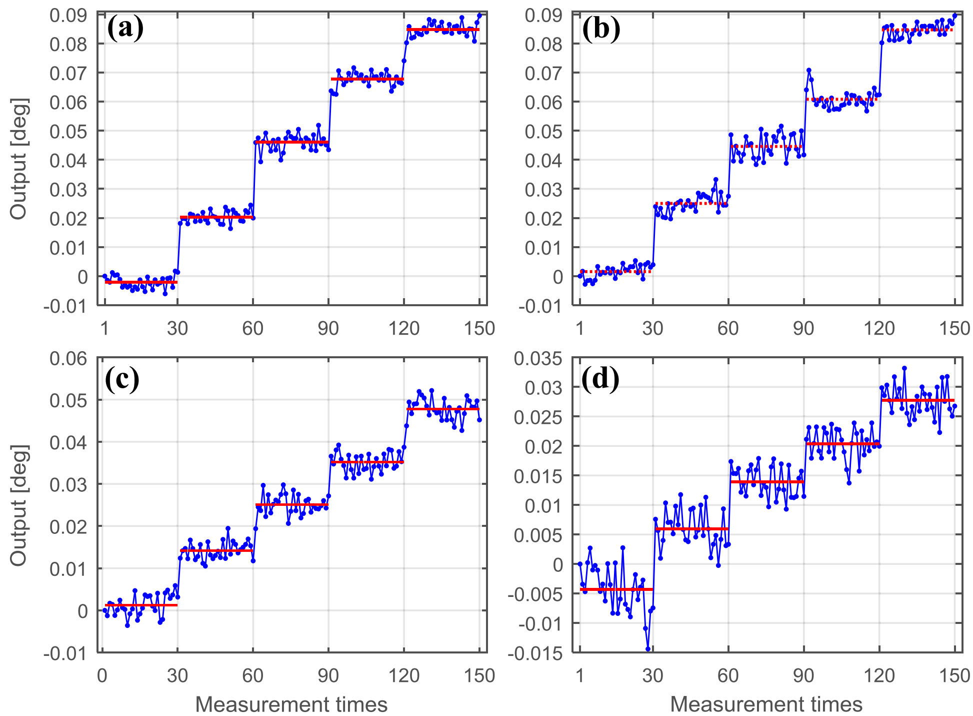

Fig. 5 (Color online) Measure roll angles as a function of input roll angles with an increment of **a** 0.02° starting from 0°; **b** 0.02° starting from 100°; **c** 0.01° starting from 0°; and **d** 0.01° starting from 160°. The output associated with each sub-figure is defined as the measured roll angle minus the corresponding starting value. The *red dotted lines* correspond to the means of 30 repeated measurements carried out for each increment of the input roll angles

elements. As shown in Fig. 5a, b, the 30 repeated measurements associated with each increment have a larger uncertainty for the starting value of 100° than that for 0°, which is in accordance with the results revealed by Fig. 4a, since the uncertainty for the input roll angle of 100° is larger than that for 0°. The main contribution to precision of the measured Stokes elements by the developed polarimeter is the shot noise of the incident light due to the relatively high output power of the employed light source (~ 100 μW at 633 nm wavelength) and the relatively low readout noise of the employed camera (1.0 e-med.) [18]. To further improve precision of the measured Stokes elements and thus measurement resolution of the developed sensor, some techniques such as weak-value and weak-value-emulated amplification and heterodyne detection [19–22] could be explored as the future work.

5 Conclusions

In summary, we have proposed a remote Stokes roll-angle sensor that measures roll angles from the detected Stokes vectors of the modulated polarized light retroreflected from a sensing unit using an LSR method. It was shown that the developed sensor could realize absolute roll angle measurement in range of 180° with a measurement resolution of better than 0.01° and a maximum absolute error of less than 0.25°. The proposed sensor adopts a coaxial design and is easy to implement and adjust. Moreover, it can be further expanded to a three-DoF angle sensor due to the sensitivity of the sensing unit to other two kinds of angles. Future work will be carried out to further improve performances of the proposed remote roll-angle sensor and reduce its size. The stability of the sensor calibration and measurement will also be examined in the future.

Acknowledgements This work was funded by the National Science Foundation of China (NSFC) (51775217, 51727809, 51525502, and 51805193), and the National Science and Technology Major Project of China (2017ZX02101006-004).

References

1. Tanner E, Granade S, Whitehead CA (2003) Autonomous rendezvous and docking sensor suite. Proc SPIE 5086:329–339
2. Arp TB, Hagedorn CA, Schlamminger S, Gundlach JH (2013) A reference-beam autocollimator with nanoradian sensitivity from mHz to kHz and dynamic range of 10^7. Rev Sci Instrum 84(9):095007
3. Billard A, Kragic D (2019) Trends and challenges in robot manipulation. Science 364:eaat8414
4. Kim JA, Kim JW, Kang CS, Jin J, Eom TB (2012) An optical absolute position measurement method using a phase-encoded single-track binary code. Rev Sci Instrum 83(11):115115
5. Gao W, Kim SW, Bosse H, Haitjema H, Chen YL, Lu XD, Knapp W, Weckenmann A, Estler WT, Kunzmann H (2015) Measurement technologies for precision engineering. CIRP Ann Manuf Technol 64:773–796
6. Liu Z, Lin D, Jiang H, Yin C (2003) Roll angle interferometer by means of wave plates. Sens Actuators A Phys 104(2):127–131
7. Qi J, Wang Z, Huang J, Gao J (2018) Resolution-enhanced heterodyne laser interferometer with differential configuration for roll angle measurement. Opt Express 26(8):9634–9644

8. Zhai Y, Feng Q, Zhang B (2012) A simple roll measurement method based on a rectangular-prism. Opt Laser Technol 44(4):839–843
9. Ploster E, Arnon S (2014) Statistics of remote roll angle measurement. Appl Opt 53(11):2437–2440
10. Li S, Yang C, Zhang E, Jin G (2005) Compact optical roll-angle sensor with large measurement range and high sensitivity. Opt Lett 30(3):242–244
11. Gillmer SR, Yu X, Wang C, Ellis JD (2015) Robust high-dynamic-range optical roll sensing. Opt Lett 40(11):2497–2500
12. Chen X, Liao J, Gu H, Shi Y, Jiang H, Liu S (2019) Proof of principle of an optical Stokes absolute roll-angle sensor with ultra-large measuring range. Sens Actuators A Phys 291:144–149
13. Tan Y, Chen C, Chen X, Du W, Gu H, Liu S (2018) Development of a tomographic Mueller-matrix scatterometer for nanostructure metrology. Rev Sci Instrum 89(7):073702
14. Goldstein DH (2011) Polarized light, 3rd edn. CRC Press, New York **Chap 16**
15. Chen X, Tao Z, Chen C, Wang C, Wang L, Jiang H, Fan D, Ekinci Y, Liu S (2018) All-dielectric metasurface-based roll-angle sensor. Sens Actuators A Phys 279:509–517
16. Zhang S, Jiang H, Gu H, Chen X, Liu S (2020) Attitude metrology based on field-of-view effect of birefringence using high-speed polarimetry. Opt Lett 45(7):2074–2077
17. Press WH, Teukolsky SA, Vetterling WT, Flannery BP (2007) Numerical recipes: the art of scientific computing, 3rd edn. Cambridge University Press, Cambridge
18. Lawall J, Kessler E (2000) Michelson interferometry with 10 pm accuracy. Rev Sci Instrum 71(7):2669–2676
19. Magaña-Loaiza OS, Mirhosseini M, Rodenburg B, Boyd RW (2014) Amplification of angular rotations using weak measurements. Phys Rev Lett 112(20):200401
20. Harris J, Boyd RW, Lundeen JS (2017) Weak value amplification can outperform conventional measurement in the presence of detector saturation. Phys Rev Lett 118(7):070802
21. Gillmer SR, Martínez-Rincón J, Ellis JD (2018) Anomalous vibration suppression in a weak-value-emulated heterodyne roll interferometer. Opt Express 26(22):29311–29318
22. He D, Xie B, Feng S (2016) Null polarimetry near shot noise limit at 1 Hz. Rev Sci Instrum 87(4):043012

Xiuguo Chen is currently an Associate professor at Huazhong University of Science and Technology. He received his B.E. in Mechanical Design Manufacturing and Automation from Shandong University of Technology in 2007, and M.E. and PhD in Mechanical and Electronic Engineering from Huazhong University of Science and Technology in 2009 and 2013, respectively. His research interests involve theory, instrumentation, and application of polarization-based techniques for nanoscale characterization and optical sensing.

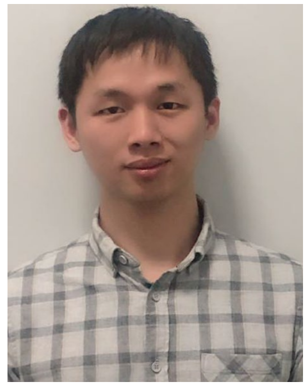

Jinbao Liao is currently a graduate student at Huazhong University of Science and Technology. He received his B.E. in Mechanical Design Manufacturing and Automation from Sichuan University in 2017. His research interest is the polarization-based optical sensors.

Honggang Gu received his B.E. in Mechanical Engineering from Huazhong University of Science and Technology in 2011, and then received his PhD in Mechanical Engineering from Huazhong University of Science and Technology in 2016. He is now working as an assistant professor at the same university with research interests in metrology and applications of ellipsometry and polarimetry.

Chuanwei Zhang is currently an Associate professor at Huazhong University of Science and Technology. He received his B.E. and ME in Mechanical Engineering from Wuhan University in 2004 and 2006 respectively, and then received his PhD in Mechanical Engineering from Huazhong University of Science and Technology in 2009. His research interests include optical techniques for critical dimension, overlay, and 3D profile metrology in nanomanufacturing.

Hao Jiang is a professor at Huazhong University of Science and Technology. In 2011, he earned his PhD in Mechanical Engineering at Florida Institute of Technology. After receiving his ultimate degree at Florida Tech, he worked as a postdoctoral research fellow and adjunct instructor at the University of Texas at Arlington until he started his appointment of Associate Professor with Huazhong University of Science and Technology in 2014. He is interested in the research topics of polarization optics based multi-parameter measurement, Micro/Nano scale mechanical variable measurement, smart/bio material based advanced metrology and computational metrology.

Shiyuan Liu is a professor of mechanical engineering at Huazhong University of Science and Technology, China, leading his Nanoscale and Optical Metrology Group with research interest in metrology and instrumentation for nanomanufacturing. He obtained his PhD in mechanical engineering from Huazhong University of Science and Technology, China, in 1998. He is a member of OSA, AVS, SPIE, and IEEE. He holds 42 patents and has authored or co-authored more than 100 papers. He was elected a Council Member of International Committee of Measurements and Instrumentation (ICMI), and was awarded the National Science Funds for Distinguished Young Scholars by the National Natural Science Foundation of China (NSFC) in 2015.